JMEPEG
DOI: 10.1007/s11665-012-0251-y

1059-9495/$19.00

Microstructure and Mechanical Properties of Direct Quenched Versus Conventional Reaustenitized and Quenched Plate

N.C. Muckelroy, K.O. Findley, and R.L. Bodnar

(Submitted April 2, 2012)

Direct quench processing of steels may be employed as a more cost efficient mechanism to produce low-carbon martensitic plate steels. However, the strengthening mechanisms of direct-quenched (DQ) steels, which can include grain size, dislocation density, and precipitation, are not well understood. Three experimental alloys containing 0.19 wt.% carbon with microalloy additions of Nb and V were developed to compare direct-quench processed steels to steels processed through reaustenitizing and quenching, the more conventional method to produce martensitic plate steels. Two different direct quench processing routes, conventional controlled rolling and recrystallization controlled rolling, with variations in the amount of final rolling reduction were investigated with two of the alloys. The third alloy was processed through reaustenitizing and quenching. The microstructures were quantified using light optical microscopy, scanning electron microscopy, and electron backscattered diffraction and correlated with tensile test results to assess the strengthening mechanisms in each of the conditions. The strength of the DQ steels was similar and matched that of the reaustenitized and quenched steel. It was found that the martensite block size was constant across the experimental conditions, and might play a major role in strengthening the DQ plates.

Keywords EBSD, martensite, steel, strengthening mechanisms, thermomechanical processing

1. Introduction

In recent years, there has been an interest in using direct-quenched (DQ) steels in place of conventional reaustenitized and quenched (RA/Q) plate. The interest stems from the prospect of reducing production costs and time by eliminating the additional reaustenitizing and cooling process. Previous research has shown that the DQ process can provide an improvement in strength without significant decrease in toughness as compared to conventional RA/Q steels (Ref 1-7). However, the mechanisms behind this phenomenon are not well understood. Furthermore, thermomechanical controlled processing (TMCP) during DQ could potentially provide strength levels that can only be attained with higher amounts of alloying in reheat quenched and tempered steels, which also decreases the overall cost of the material. Therefore, a better understanding of the dominant strengthening mechanisms in DQ steel is necessary to assess the potential for large-scale DQ plate steel production.

The conventional RA/Q process consists of hot rolling and air cooling followed by reaustenitization and water quenching, which results in equiaxed prior austenite grains; the microstructure is typically tempered to improve toughness. Two DQ processes that have been studied in detail are controlled-rolled and direct-quenched (CR + DQ) and recrystallization-controlled-rolled and direct-quenched (RCR + DQ). The CR + DQ process consists of roughing passes at high temperature and finish rolling below the austenite recrystallization stop temperature (T_R), followed by quenching in water. As finish rolling occurs at a temperature below the austenite recrystallization stop temperature, austenite grains are "pancaked," or elongated, in the rolling direction (RD) prior to quenching. Since recrystallization is suppressed, there should be a high degree of retained deformation substructure within the austenite prior to quenching. The presence of these additional dislocations (and their corresponding strain fields) can decrease the energy required to nucleate martensite on cooling, and may be a mechanism that leads to a finer final microstructure than that achieved by traditional RA/Q steels (Ref 8). The increase in deformation substructure may also provide nucleation sites for microalloy precipitates during processing. The RCR + DQ process consists of roughing passes at high temperature and finish rolling just above the austenite non-recrystallization temperature, followed by quenching in water. The prior austenite grains are equiaxed and small.

The strength of materials produced using reaustenitizing and quenching without tempering is usually lower than those of the same alloy composition after direct quenching, though the difference diminishes as the carbon content approaches 0.2 wt.% (Ref 3). The ductility and impact toughness are higher in RA/Q steels (Ref 1, 3, 9, 10). Weiss (Ref 11) observed that the strength difference between the RA/Q and DQ processed steels exists in both the as-quenched and tempered conditions, which suggests that the tempering response may also be altered through DQ processing. Taylor found similar

N.C. Muckelroy and **K.O. Findley**, Department of Metallurgical and Materials Engineering, Colorado School of Mines, 1500 Illinois St., Golden, CO 80401; and **R.L. Bodnar**, SSAB Americas, 1755 Bill Sharp Blvd., Muscatine, IA 52761. Contact e-mails: nika.muckelroy@gmail.com, kfindley@mines.edu, and rick.bodnar@ssab.com.

Published online: 30 May 2012

results in a study of low-carbon (0.10-0.19 wt.%) experimental microalloyed steels, concluding that controlled rolling and direct quenching increases strength (Ref 1). Similarly, Foley and Krauss found that an ASTM A514 steel with vanadium processed with a low finish rolling temperature, i.e., CR processing, possessed the best combinations of strength and ductility in both as-quenched and tempered states (Ref 4). These properties were shown to correlate with martensite packet size; however, martensite packet size has not been definitively shown to be the sole mechanism that controls the final properties in these steels (Ref 5).

There are several strengthening mechanisms operative in martensitic steels. It is hypothesized that the strength difference between DQ and RA/Q steels is due to differences in martensite substructure (packet, block, and lath) size, amount of retained strain, and microalloy precipitation. It is intuitive that TMCP may change the amount of dislocation substructure and density, thereby increasing the martensite strength. Direct-quench processes alter the prior austenite grain size (PAGS) and morphology and possibly introduce deformation substructure. DQ specimens with an inherited austenite defect structure (CR + DQ) and recrystallized prior austenite grains (RCR + DQ) both exhibit higher strength than the RA/Q condition; therefore, martensite inheritance of the austenite defect structure cannot be the only explanation for the strength increase. Any change in the alloying or processing that increases the precipitate volume fraction will also increase strength. Microalloy precipitates can form during TMCP and during tempering. Finally, if TMCP processing results in a finer microstructure, there should be a resulting increase in strength. The basic unit of low-carbon martensitic microstructures is a martensite lath. Groups of laths with the same habit plane compose a martensite packet. Within a packet, adjacent laths with the same variant or variants within approximately 10 degrees of misorientation compose blocks. Theoretically, martensite blocks are composed of very specific combinations of variants with low misorientation (Ref 12). While most researchers have examined the effect of martensite packet size on yield strength, Morito (Ref 13) determined that a Hall-Petch relationship exists between martensite block size and yield strength in low-carbon steels. Martensite blocks are the smallest microstructural units divided by high-angle grain boundaries, so they may be considered as the effective grain size in the material.

The objective of this study is to further elucidate the operative strengthening mechanisms in TMCP DQ plate steels in the as-quenched condition by using different finish rolling conditions and then assessing the resulting tensile properties and martensite microstructure. Specifically, the effects of the amount of finish rolling reduction and the martensite block size on strength in DQ and RA/Q plate steels were examined. While tempering is typically performed after quenching, except in steels with designed autotempering response, the focus of this investigation is on the as-quenched strengthening mechanisms. Strength increases in DQ steels relative to RA/Q steels during tempering have largely been attributed to precipitate strengthening (Ref 3, 9). A better understanding of the differences in strength before tempering could help optimize processing of DQ steels for either autotempering or tempering after quenching.

2. Experimental Procedures

2.1 Alloy Development and Processing

Three experimental alloys (CSM steels) were designed based on ASTM A514 steels. Although the compositions meet ASTM A514-Grade S, which is typically used in structural applications, such compositions in the as-quenched or quenched and lightly tempered (to lower quenching stresses) conditions may also be appropriate for abrasion applications. The alloy compositions were established to produce alloys processed through CR, RCR, or RA/Q with similar PAGS. The alloys were also produced to meet a common industry carbon equivalence standard of 0.48 maximum, calculated from the International Institute of Welding (IIW) carbon equivalence equation (Eq 1),

$$C_{eq} = C + \frac{Mn}{6} + \frac{Cr + Mo + V}{5} + \frac{Ni + Cu}{15} \quad \text{(Eq 1)}$$

where all values are in wt.%. The alloys are designated as RCR (for recrystallization-controlled-rolled), CR (for controlled-rolled), and RA/Q (for reaustenitized and quenched). The RCR steel was designed to have a low non-recrystallization temperature, T_{nr}, with an addition of 0.06 wt.% vanadium (V) so that rolling above this temperature could be easily achieved. The non-recrystallization temperature is the temperature below which complete recrystallization cannot occur (Ref 14). T_{nr} was used to determine the finish rolling temperature rather than T_R because it is easier to measure T_{nr} and there are many available empirical equations to relate T_{nr} to composition and processing. The CR steel was designed to have a relatively high T_{nr} by means of a 0.033 wt.% Nb addition, so finish rolling below this temperature could easily be achieved without dropping below the A_{r3} temperature. The RA/Q steel was designed with a 0.019 wt.% Nb addition for austenite grain size control during processing. Using a relatively high-carbon content of 0.19 wt.% ensured a fully martensitic microstructure to eliminate any effects from non-martensitic constituents on mechanical behavior. All of the alloys had a stoichiometric ratio of Ti to N, so both components were completely tied up in TiN precipitates. The chemical compositions of all the alloys studied are presented in Table 1.

The processing schedule for each of the DQ specimens, described in detail below, involved roughing passes at a high temperature where the alloy elements were in solution in austenite with the exception of titanium nitrides followed by finish rolling either above or below the T_{nr}. The T_{nr} of each alloy was estimated using two different empirical equations. One of the most commonly used calculations of the T_{nr} as a

Table 1 Chemical composition, in wt.%, of the steels examined

Steel	C	Si	Mn	Mo	V	B	P	S	Ti	Al	N	Nb	Cu	Ni	Cr	C_{eq}
RCR	0.19	0.24	1.24	0.12	0.06	0.0015	0.003	0.002	0.015	0.031	0.005	0	0.15	0.13	0.13	0.48
CR	0.19	0.23	1.24	0.12	0	0.0014	0.003	0.002	0.016	0.032	0.005	0.033	0.15	0.13	0.13	0.47
RA/Q	0.19	0.24	1.23	0.11	0	0.0013	0.004	0.002	0.016	0.022	0.005	0.019	0.14	0.13	0.13	0.46

function of alloy composition was developed by Boratto et al. (Ref 14):

$$T_{nr} = 887 + 464 \cdot C + (6445 \cdot Nb - 644 \cdot \sqrt{Nb}) + (732 \cdot V - 230 \cdot \sqrt{V}) + 890 \cdot Ti + 363 \cdot Al - 357 \cdot Si \quad \text{(Eq 2)}$$

Seventeen different alloys, processed with a strain per pass of 0.2, were used to develop the equation.

More recently, a model that includes strain per pass as a variable in the T_{nr} equation was developed by Fletcher (Ref 15):

$$T_{nr} = 203 - 310 \cdot C + 657 \cdot \sqrt{Nb} + 149 \cdot \sqrt{V} + 683 \cdot \exp(-0.36 \cdot \varepsilon) \quad \text{(Eq 3)}$$

Fletcher fit the equation to T_{nr} data from 17 alloy steels, corresponding to 59 different T_{nr} values, with carbon contents between 0.04 to 0.18 wt.% and processed with soaking temperatures of 1150-1260 °C, interpass times of 16-40 s, pass strains of 0.15-0.30, and a strain rate approximately equal to 1 s^{-1}. There is a caveat to Fletcher's analysis; the sign on the carbon term is negative, which is counterintuitive because increased carbon will increase the amount of precipitation that inhibits recrystallization and thus increase T_{nr} as opposed to decrease T_{nr} as Eq 3 predicts.

Equation 2 and 3 were used to estimate T_{nr}, and the results are shown in Table 2. The strains per pass in the last three columns are the strains per pass for the finish rolling used in the investigation, which is described later. The Boratto equation predicts the largest values of T_{nr}, while Eq 3 predicts much lower values of T_{nr}. Equation 3 was used to determine the finish rolling temperatures for the CR and RCR conditions since it was developed for a larger range of alloys and process conditions than the Boratto equation. When the strain per pass is assumed to be 0.13 or greater in Eq 3, the T_{nr} is <850 °C for the RCR alloy and much >850 °C for the CR alloy. Therefore, a finish rolling temperature of approximately 850 °C was selected for both the RCR and CR plates.

Production of the experimental plates began with casting one 12.7 × 12.7 × 25.4 cm^3 (5 × 5×10 $in.^3$), 45.4 kg (100 lb), ingot of each chemistry at the ArcelorMittal Research Center (East Chicago, IL). Each of the ingots was hot rolled by US Steel Research and Technology Center (Munhall, PA) to 7.62 cm (3 in.) thick and air cooled before further processing. Thermocouples were inserted into the mid-thickness of the slab or mults cut from the slabs to monitor temperature during subsequent hot rolling and finish rolling. The RA/Q plate was reheated to 1250 °C for 1.5 h, rolled to the final 15 mm (0.6 in.) thickness, and air cooled. It was then reaustenitized at 950 °C for 1 h and quenched in water. The CR and RCR plates were cut into three mults of equal length that were to eventually be finish rolled to either 40%, 55%, or 70% final reduction. First, the three sections were reheated to 1250 °C for 1.5 h and rolled to different intermediate thicknesses so each plate would have the same final thickness of 15 mm (0.6 in.) after finish rolling. Using Irvine's solubility product equation for NbC (Ref 16), the solution temperature for NbC in the CR and RA/Q conditions is 1244 and 1167 °C respectively. Thus, the reheat temperature of 1250 °C was sufficient to put the Nb and C in solution before further processing in both conditions.

Table 2 Calculated T_{nr} in degrees Celsius for the RCR and CR alloys

	Boratto (Eq 2)	0.13 ε/pass (Eq 3)	0.18 ε/pass (Eq 3)	0.23 ε/pass (Eq 3)
RCR	901	831	820	808
CR	1019	915	904	892

The DQ mults were then air cooled to the finish rolling temperature and rolled to either 40, 55, or 70% final reduction in three passes, followed by direct quenching with water jets. The average percent reduction per pass during finish rolling was 12.5, 16.75, and 20.8% for the 40, 55, and 70% final reduction conditions, respectively (Table 2). The corresponding true strain per pass for each condition, which was input into Eq 3, was 0.13, 0.18, and 0.23, respectively. The force of water jets caused the plates from the RCR conditions rolled with 55 and 70% final reductions to be ejected from the line during quenching, which resulted in a much lower and less uniform cooling rate compared to the other plates. Thus, in this article, only results from the CR40, CR55, CR70, RCR 40, and RA/Q conditions will be discussed. The average cooling rates on quenching in these conditions, determined between 150 and 750 °C, ranged from 40 to 60 °C/s.

2.2 Microstructural Analysis

Metallography samples were taken from each plate to show both the transverse and longitudinal planes with respect to the RD. A polishing procedure that excluded the use of water-based polishing compounds and extenders was developed because the alloys proved extremely sensitive to water-based products. The experimental samples were etched using a 4% picral-1% HCl-1% Teepol solution to reveal the martensite microstructure. The samples were also etched to reveal the prior austenite grains using a boiling 6% picral-1%-HCl-1% Teepol solution containing boiling stones. Light optical microscopy, scanning electron microscopy (SEM), and electron backscattered diffraction (EBSD) were performed on the metallography samples to characterize the overall grain structure and the martensite substructure for correlation to mechanical properties. Data obtained from EBSD were used to quantitatively determine the martensite block size for each condition. The scans were set to index ferrite Kikuchi bands rather than martensite, as there is less than a 1% difference in lattice parameters between the martensite bct and ferrite bcc crystal structures for 0.19 wt.% C steels, which is less than the resolution of the EBSD scans. Scanning for ferrite rather than martensite also eliminates an artifact in the EBSD data, which misinterprets the [100]/90° relationship between the *c* and *a* axes within the martensite crystal as high-angle boundaries. Ten areas of 75 × 75 μm^2 in size were evaluated with a 0.17 μm step size and were used in order to both optimize scan time and capture all relevant elements of the microstructure. Two grain dilations were performed on the resulting data, with a minimum grain size threshold of 2 pixels; grains composed of 2 pixels or less were excluded from the analysis. A systematic study was performed on the EBSD data using four different minimum grain sizes (2, 5, 7, and 10 pixels), and it was found that varying the minimum grain size did not significantly affect the results of subsequent block size measurements.

The PAGS of the etched samples and the block size from EBSD scans were determined using the cycloid method for estimating grain size in anisotropic materials outlined by

Morris et al. (Ref 17). A cycloid is the locus of a point on the rim of a circle of radius a rolling along a straight line. According to Baddeley et al. (Ref 18), performing grain boundary intersection counts on metallography sections oriented vertically (parallel to the RD and perpendicular to the rolled surface of the plate) using test lines of cycloid shape (rather than straight lines) that are oriented such that the minor axis of the cycloid is parallel with the vertical axis gives an unbiased estimate of the grain size. The parametric equations that describe the cycloid are:

$$Y = a\,[1 - \cos(\theta)] \quad \text{(Eq 4)}$$

$$X = a\,[\theta - \cos(\theta)] \quad \text{(Eq 5)}$$

where $0 \leq \theta \leq \pi$ and a is taken as 1. The sampling error resulting from single vertical plane measurements is significantly lower than that for the ASTM method (which uses three orthogonal test lines), even if twice as many measurements are performed for the ASTM procedure (Ref 18). Therefore, the efficiency of the single vertical plane sampling technique is significantly higher than that of the ASTM procedure (Ref 17).

The cycloid method was chosen to estimate grain size because it provides a method to compare unbiased grain size measurements for both elongated and equiaxed microstructures. Unbiased measurements of grain size are important to compare the strengthening increment and microstructural evolution associated with austenite grain size in the selected process conditions. As shown in the "Results and Discussion" section, the resulting austenite grain sizes from the various processing conditions represent a range of pancaked and equiaxed grains.

2.3 Mechanical Testing

Tensile testing was performed according to ASTM E8 (Ref 19) using a 5.08 cm (2 in.)-50% extension Shepic brand extensometer at room temperature (approximately 23 °C) with constant crosshead velocity of 2.54 mm/min (0.1 in./min). Two to four full thickness flat tensile specimens were taken in each orientation from each of the CR and RCR plates. Data obtained from tensile testing were used to determine ultimate tensile strength, 0.2% offset yield strength, uniform elongation, and total elongation. The uniform elongation was determined using Considere's construction. The tensile specimen dimensions are shown in Fig. 1. All of the tensile specimens taken from the laboratory-produced plates were machined to a thickness of 3.18 mm (0.125 in.).

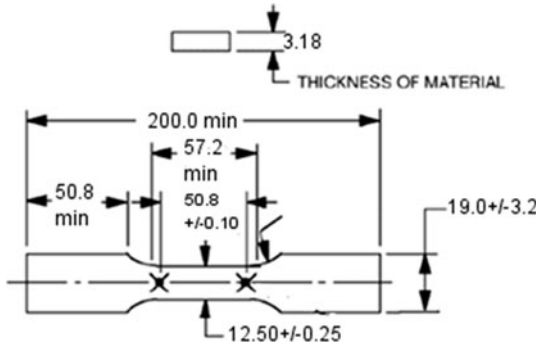

Fig. 1 Schematic showing sample dimensions of the tensile specimens. All dimensions are in mm

3. Results and Discussion

3.1 Effect of Thermomechanical Controlled Processing Route on Microstructure

TMCP during direct quench processing changed the prior austenite grain morphology. The prior austenite grain structure is shown in Fig. 2 for the CR40, CR55, CR70, RCR40, and RA/Q conditions; the RD and normal direction (ND) are shown in Fig. 2(a). The prior austenite grains in the RA/Q condition are equiaxed, while the CR and RCR conditions have prior austenite grains that are pancaked to some degree. The majority of the austenite grains in the RCR40 condition are slightly elongated, though about 40% of the austenite grains are equiaxed and recrystallized. The austenite grains are the most elongated in the CR70 condition. The austenite grains are equiaxed in the RA/Q condition.

The presence of elongated grains in the RCR40 condition suggests that the finish rolling temperature only allowed for partial recrystallization of the deformed austenite grains in contrast to the prediction of Eq 3. The mixed microstructure of pancaked and recrystallized grains implies the finish rolling temperature was likely between the T_{nr} and T_R. In general, T_R is 75 °C below T_{nr} (Ref 20). Therefore, the Boratto equation, which predicts the T_{nr} to be 901 °C and thus an approximate T_R of 825 °C, appears to be the more accurate prediction for this steel.

SEM images of the martensitic microstructure of the five conditions are shown in Fig. 3; the RD and ND are shown on Fig. 3(a). The microstructure becomes visibly finer with increasing amounts of reduction in the CR conditions. The size scale is also finer in the CR55 and CR70 conditions than it is in the RCR40 and RA/Q conditions. Kaijalainen et al. (Ref 21) reported a refinement of martensitic and bainitic laths with increasing reduction levels during TMCP processing. This result is supported by the earlier discussion about dislocation substructure, retained from TMCP processing, reducing the energy for martensite nucleation so the martensite laths become finer. The features in the images shown in Fig. 3 are larger than the martensite lath size, and they are more likely martensite blocks. Weiss (Ref 11) also observed a qualitative refinement of the microstructure for DQ processed steel compared to RA/Q steel, but the measured size of martensite laths and blocks was approximately the same for all of the conditions. As discussed later, a similar result was found in this study. Thus, even though the martensitic microstructure may appear finer due to DQ processing, it is not necessarily quantitatively finer. The appearance of a difference in microstructure size scale may be due to differences in microstructure morphology, particularly the martensite blocks, which results from different degrees of austenite pancaking during TMCP.

EBSD scans showing inverse pole figures overlaid onto image quality maps are presented for the DQ steels in Fig. 4. High-angle grain boundaries with misorientation angles >15° are also shown in yellow on the figure. Each color of the inverse pole figure map represents a different crystallographic orientation of the martensite structure, indicated by the key in Fig. 4. Martensite laths are not distinguished in the inverse pole figure maps because the laths have a similar orientation within each martensite block. The martensite blocks are separated by high-angle grain boundaries. Thus, the martensite block size is

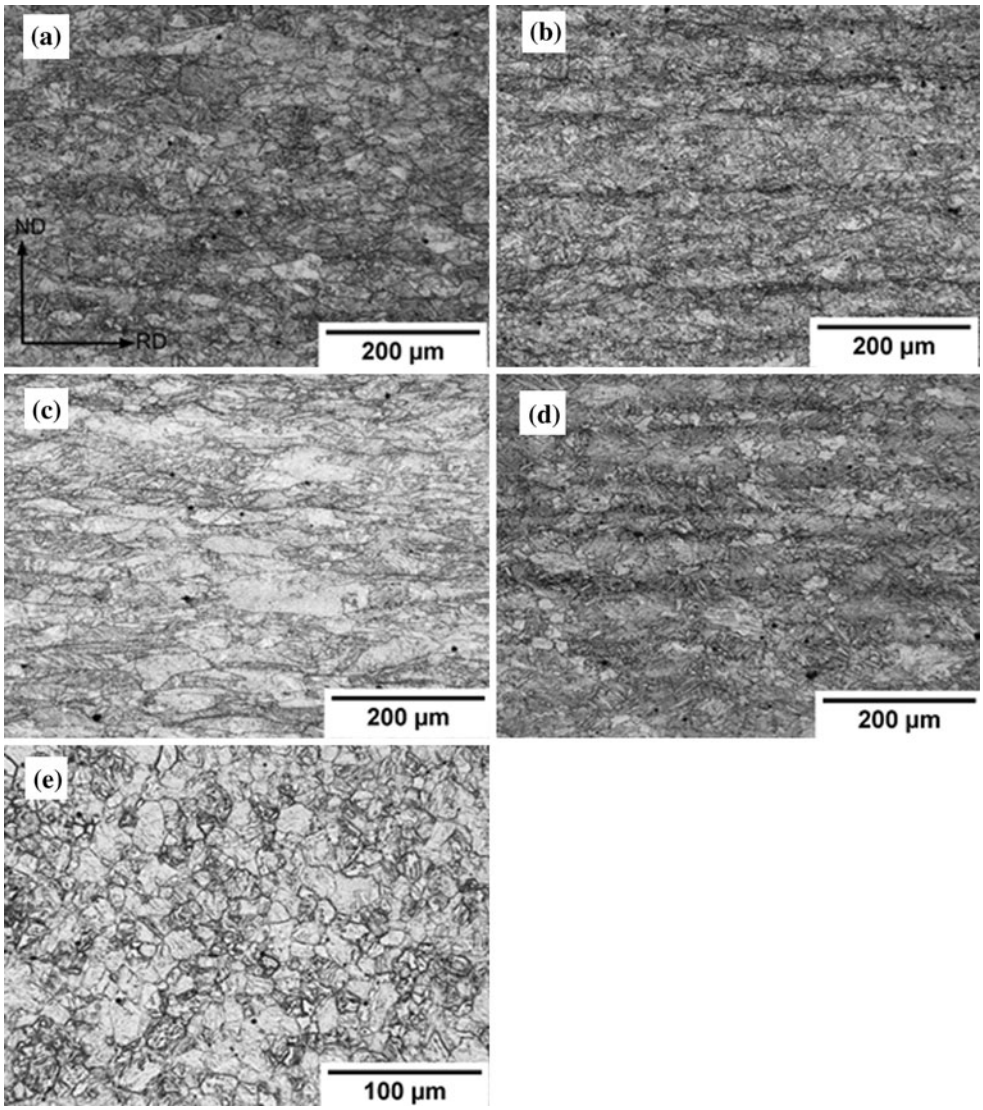

Fig. 2 Prior austenite grains in (a) CR40, (b) CR55, (c) CR70, (d) RCR40, and (e) RA/Q conditions

potentially the effective grain size for strengthening. The block morphology obviously changes as a function of the deformation conditions. Martensite blocks in the CR conditions appear to have a higher aspect ratio than the more equiaxed blocks in the RCR and RA/Q conditions, though they do not appear to be aligned or oriented in the RD.

The PAGS and the block sizes are shown in Table 3. Increasing the amount of reduction during controlled rolling decreases the PAGS from 30.6 μm for the 40% finish rolling condition to 15.7 μm for the 70% finish rolling condition. Recrystallization controlled rolling results in a finer PAGS of 9.9 μm for the RCR 40 condition. The reaustenitizing and quenching process resulted in the finest PAGS of 6.9 μm. However, the block size is seemingly insensitive to the PAGS for this range of grain sizes. Although the microstructure appears finer in the larger reduction CR conditions compared to the RCR and RA/Q conditions in the SEM micrographs, the measured microstructure size scale is comparable for all of the conditions as discussed previously. Similarly, Morito et al. (Ref 13) found that block size only varies by a factor of 2 over a PAGS range that spans from approximately 5 to 350 μm. The block size data are also consistent with Morito's findings that Mn additions decrease the effect of PAGS on martensite block size and decrease the magnitude of the block size compared to plain carbon steel. Adding solid-solution alloying elements such as Mn may harden the austenite and lower the M_S temperature, thus making it more difficult for strain in the austenite to accommodate the martensite transformation; the result is a finer block size (Ref 13). The block size distribution, measured using TSL OIM™ Image Analysis software, also was very similar for all of the investigated conditions.

3.2 Effect of Thermomechanical Controlled Processing on Tensile Behavior

The tensile behavior of the CR, RCR, and RA/Q plates is similar in both the longitudinal and transverse directions with some exceptions (Fig. 5 and 6). The yield strength decreases in the controlled rolling conditions from 40 to 55% finish rolling reduction and then increases again for the 70% finish rolling reduction, though the yield strength differences are within the range of data scatter for each condition. A similar trend in hardness and yield strength was observed by Kaijalainen et al. (Ref 21) in controlled-rolled steel with a lower carbon content

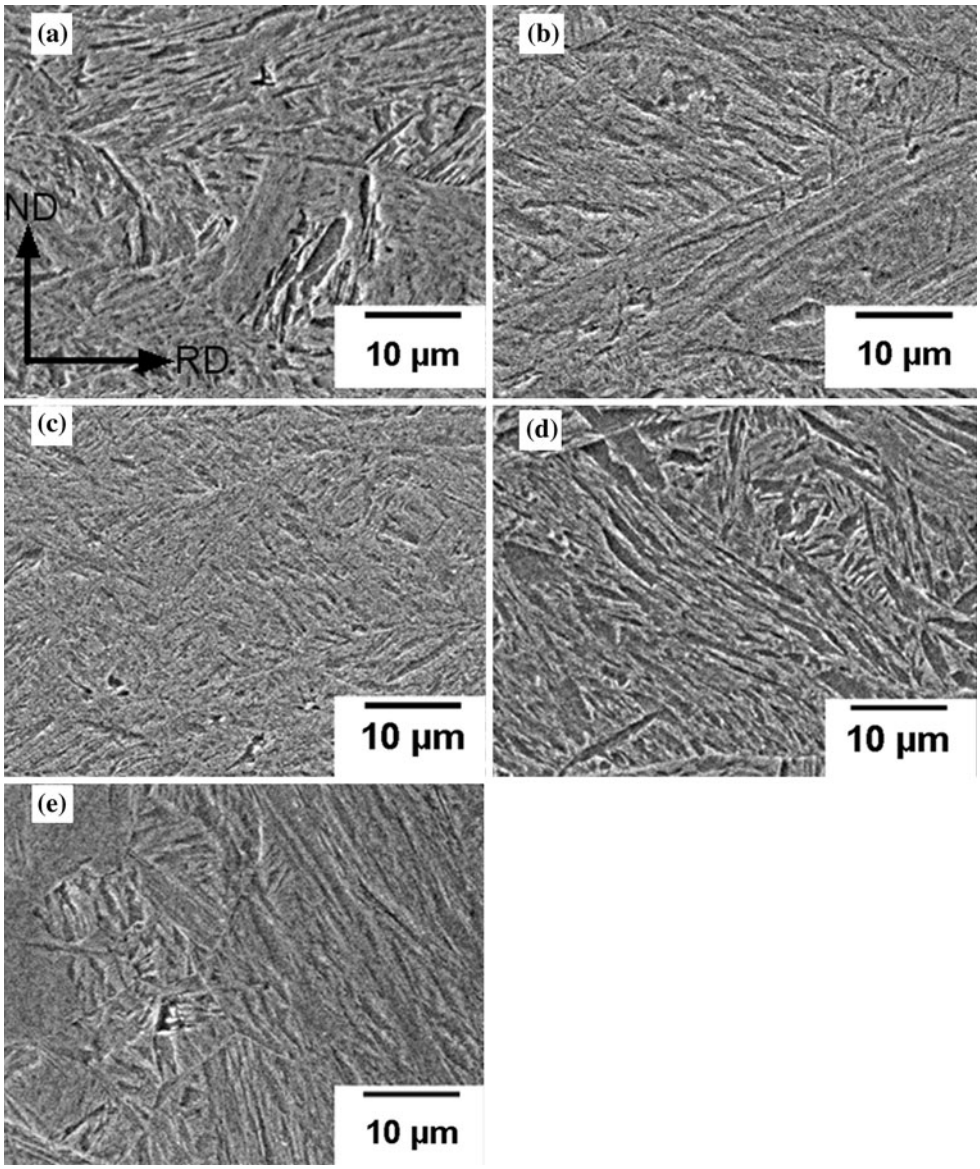

Fig. 3 SEM images of the martensitic microstructure in (a) CR40, (b) CR55, (c) CR70, (d) RCR40, and (e) RA/Q conditions

over a slightly smaller range of finish rolling reductions. The dip in strength at 55% finish rolling reduction is not as apparent in the ultimate tensile strength data. The transverse specimens nearly always possess higher yield and tensile strengths in the CR steels. This was also observed by Weiss in direct quenched and tempered steels (Ref 11) and by Kaijalainen et al. (Ref 21) and may be related to specimen texture effects. If the martensite block size is a prominent strengthening mechanism, the degree of anisotropy should be low because the martensite blocks are not locally aligned in a preferential direction with respect to the RD. However, the presence of anisotropy with transverse strengths greater than longitudinal strengths in the CR conditions suggests that there may be macroscopic texture associated with the TMCP. Very little if any anisotropy is present in the RCR and RA/Q conditions, which implies that anisotropy in strength is a result of austenite conditioning below the T_R. Reaustenitizing and quenching produced the most uniform microstructures as exhibited by the small amount of scatter in yield strength and tensile strength. The uniform and total elongation are also very similar across all of the conditions. The only exception is that the RA/Q steel has a higher total elongation and slightly higher uniform elongation than the DQ steels.

The yield and tensile strength data from the DQ plates exhibits a large amount of scatter. The processed plate and the gripped portions of the fabricated tensile specimens were characterized using Rockwell hardness tests before tensile testing. Several locations in the CR and RCR plates had low Rockwell C hardness values well below 45HRC, the expected value for a martensitic microstructure with 0.19 wt.% carbon. This indicated that the thermomechanical processing across the experimental plates was not uniform and that non-martensitic constituents such as bainite may have been present in some areas. Tensile specimens with a low Rockwell hardness reading obtained from the gripped regions were not used in the results, but there could be some localized regions with non-martensitic constituents in the gage sections of tested specimens that contributed to the scatter in tensile properties. Weiss (Ref 11)

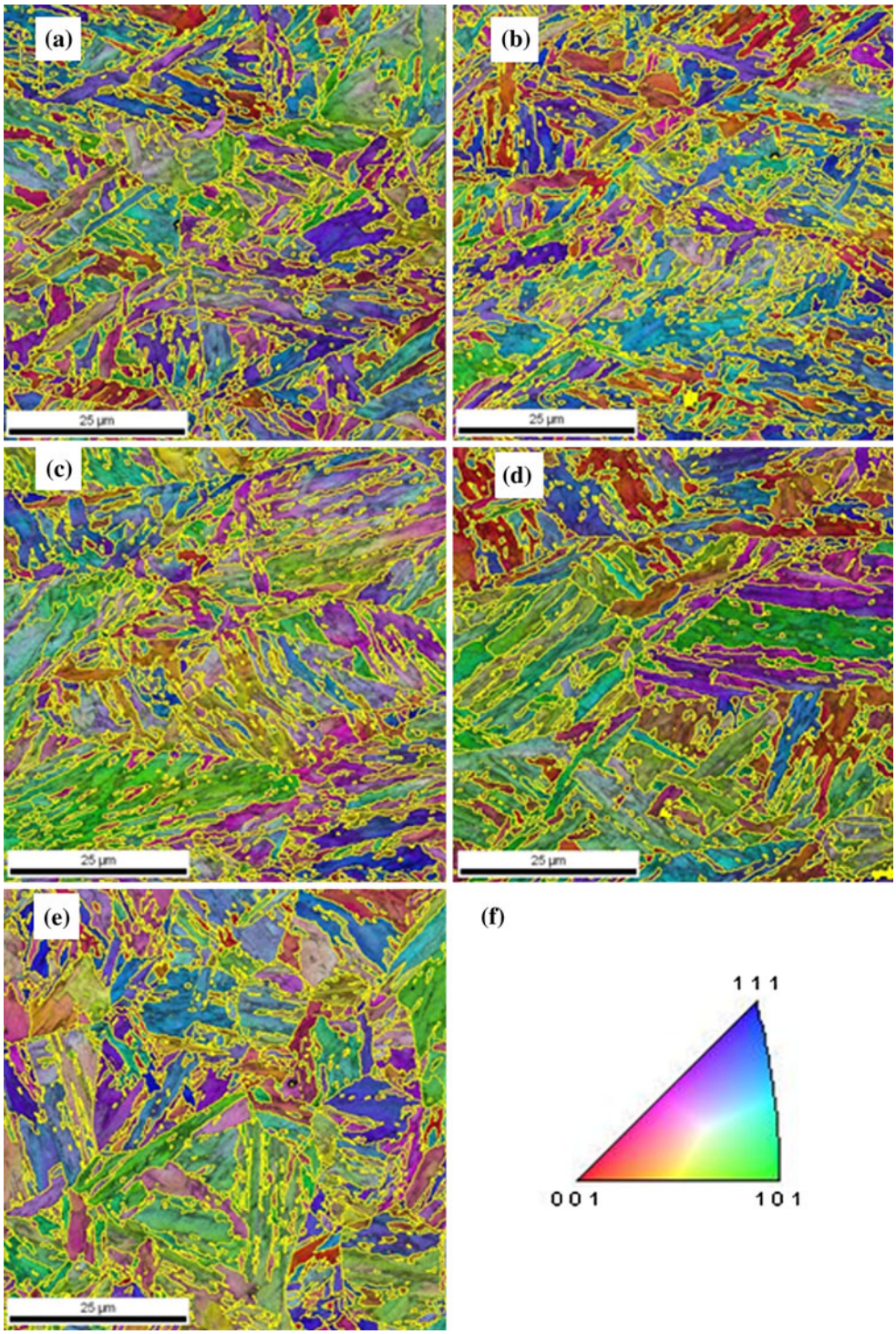

Fig. 4 EBSD inverse pole figure maps of the martensitic microstructure in (a) CR40, (b) CR55, (c) CR70, (d) RCR40, and (e) RA/Q conditions. High-angle grain boundaries are outlined in yellow. (f) Pole figure key used for the inverse pole figure maps (colour figure online)

Table 3 Prior austenite grain size and martensite block size resulting from each processing condition

	CR40	CR55	CR70	RCR40	RA/Q
PAGS, µm	30.6	20.7	15.7	9.9	6.9
Block size, µm	1.25	1.24	1.21	1.20	1.23

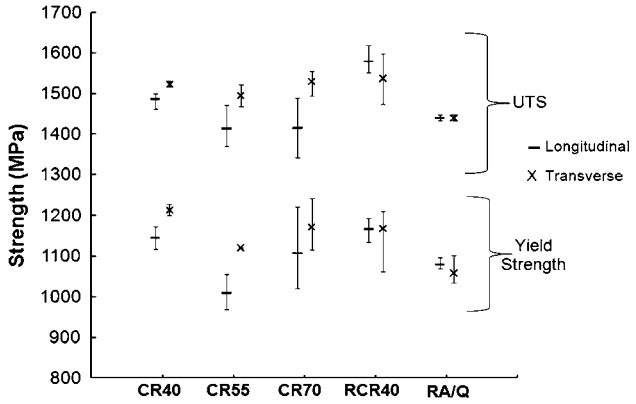

Fig. 5 Yield and tensile strengths of the CR, RCR, and RA/Q steels in the longitudinal and transverse orientations with respect to the RD

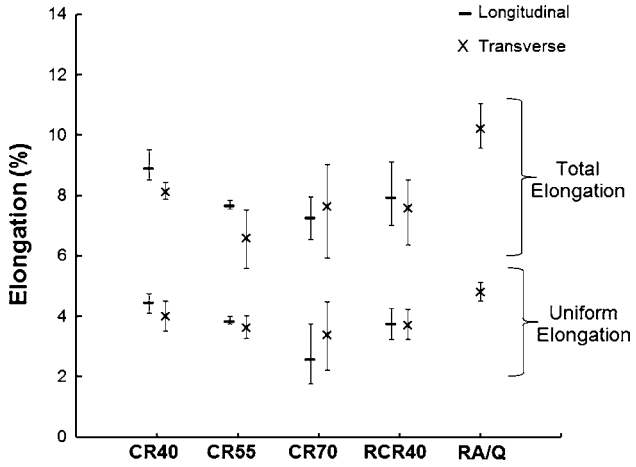

Fig. 6 Uniform and total elongations of the CR, RCR, and RA/Q steels in the longitudinal and transverse orientations with respect to the RD. The data from the RA/Q longitudinal orientation is not shown because it is very similar to the transverse orientation data

found small amounts of bainite in RCR steel with a similar carbon level, and Kaijalainen (Ref 21) found bainitic transformation products in DQ steel, though the steel had a much lower carbon level than the steels in the present investigation. The scatter in properties may be inherent in direct quench processing that results in as-quenched martensitic microstructures. Weiss (Ref 11) also observed scatter in strength data in CR and RCR DQ experimental plates with up to approximately 150 MPa variation. Kaijalainen (Ref 21) did not observe as much scatter in strength, but also reported mixed microstructures of with significant amounts of bainite in addition to the martensite.

The scatter in the data may mask some differences in strength, but the results at least show that DQ processing can be employed to achieve similar or higher strength levels to RA/Q steels without the additional reheating and quenching step, even with variation in properties across the plate that might be inherent in DQ processing. Overall, the tensile properties are largely independent of the processing conditions (i.e., finish rolling reduction, controlled rolling versus recrystallization controlled rolling versus reaustenitizing and quenching) over the range of processing conditions that were assessed. If deformation substructure is responsible for strengthening in the CR conditions, it would be expected that 70% final rolling reduction would result in the highest strength and 40% would result in the lowest strength, but this is not the case. The RCR40 and RA/Q steels, which should have less deformation substructure, are similar in strength to the CR steels. Together, these results suggest that other strengthening mechanisms strongly affect mechanical properties.

3.3 Discussion of Operative Strengthening Mechanisms in DQ and RA/Q Steels

The strength and ductility of each condition is comparable but the prior austenite grain structures are significantly different. Thus, either the strengthening mechanisms including block size, deformation substructure, solid solution strengthening, or precipitation, are present in different magnitudes for each condition, or there is one dominant strengthening mechanism that has a comparable influence across all the conditions. The following section will examine the effects of three possible strengthening mechanisms: grain size, precipitate, and dislocation substructure strengthening.

The block size of a martensitic steel alloy may be the effective grain size, as the blocks are the smallest microstructural unit separated by high-angle boundaries (Ref 12, 13). However, according to Morris (Ref 22), due to the limited number of Bain variants, it is likely that some adjacent blocks are oriented so the Burgers vector is conserved for dislocations passing between the blocks. Therefore, the effective grain size may be some small multiple of the actual block size. The 0.2% offset yield stress was determined for the DQ and RA/Q steels and plotted against block size in a Hall-Petch type plot (Fig. 7). These data are compared to the data and Hall-Petch relationship derived by Morito et al. (Ref 13) for steel with a similar carbon content but no microalloying. The results from the DQ and RA/Q plates fall within the range of Morito's data and Hall-Petch relationship, suggesting that block size plays a role in strengthening in these DQ alloys. The average yield strengths of the CR40, CR70, CR55 transverse orientation, and RCR40 conditions are above the Hall-Petch trend line compared to the CR55 longitudinal orientation and RA/Q conditions. Therefore, there may be additional strengthening mechanisms due to TMCP that provide a small boost of strength. The importance of block size is evident because Morito's data was obtained from a steel alloy with very few alloy additions other than carbon and manganese to provide strength and it was not subjected to TMCP processing; however, the material still has comparable strengths for similar block sizes to the microalloyed and TMCP-processed steel from this study. The austenite grain size has also been suggested to correlate to strength. However, the strength of the DQ alloys in this investigation is independent of PAGS. In fact, the material with the lowest PAGS, the RA/Q condition, has strength levels on the lower end of the strength deviation for 3 of the 4 DQ conditions with larger PAGS. The dependence of strength on PAGS or block size may be related to both alloy and processing conditions that promote different types of boundary strengthening.

Precipitation strengthening due to the Nb and V microalloy additions must also be considered. Figure 8 shows the solubility product curve for $NbC_{0.87}$ (Ref 23). The figure shows that since all finish rolling was performed below 1150 °C in the controlled-rolled condition, precipitation of NbC occurred during rolling. This allowed for effective pinning of the prior

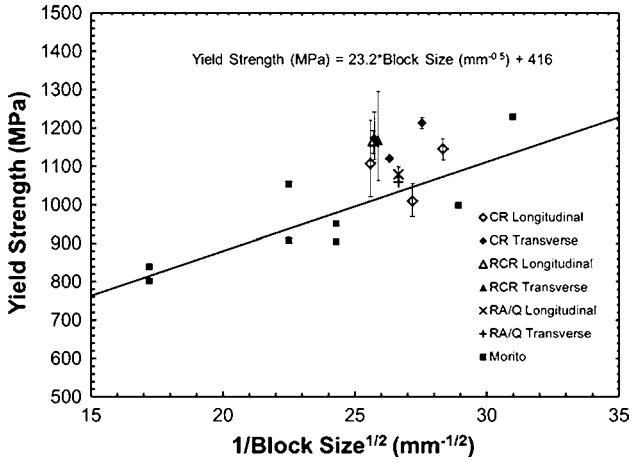

Fig. 7 Yield strength vs. block size for the DQ and RA/Q processed steels in this study compared to data and a derived Hall-Petch relationship from Morito et al. [13]

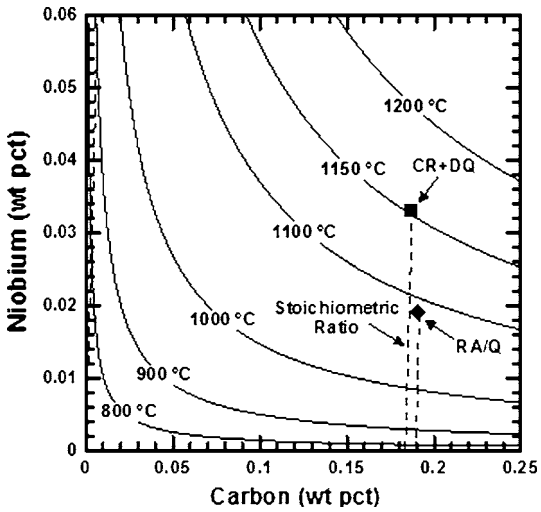

Fig. 8 Solubility product curves for niobium carbide ($NbC_{0.87}$) in austenite. Compositions of the experimental steels are plotted along with the stoichiometric ratio for $NbC_{0.87}$

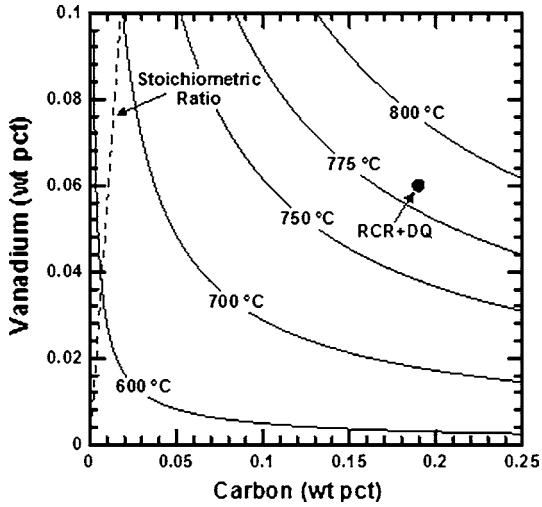

Fig. 9 Solubility product curves for vanadium carbide ($VC_{0.75}$) in austenite. Compositions of the experimental RCR steel are plotted along with the stoichiometric ratio for $VC_{0.75}$

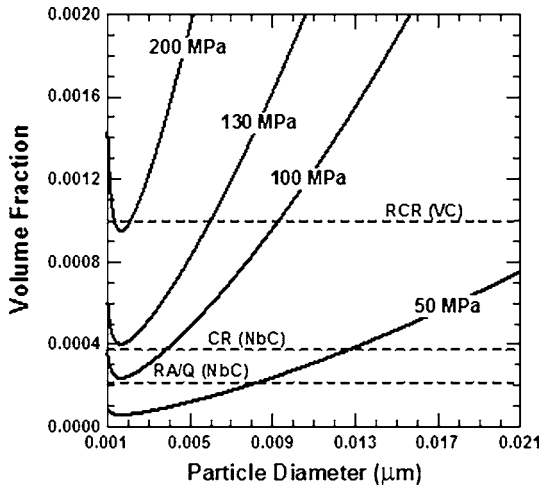

Fig. 10 Plot of volume fraction of precipitates vs. particle diameter for various strengthening increments. The theoretical maximum volume fraction of precipitates for the experimental steels was calculated from Gladman (dotted lines) [23]

austenite grain boundaries, preventing recrystallization of the austenite at higher temperatures; the NbC also provides precipitate strengthening. The RA/Q steels also contain Nb additions, which results in precipitation during the air cooling step before reaustenitizing. Hansen et al. (Ref 24) observed Nb(C,N) precipitates on the order of 5 nm in steels of comparable composition after solutionizing at 1250 °C, cooling directly to 950 °C and holding for 5 min, hot rolling in a single pass, and then reheating to 950 °C for times up to 10,000 s before quenching. Precipitates of this size would certainly provide strengthening if present even in small volume fractions. However, the precipitates likely coarsen during the reheating step from room temperature to 950 °C, reducing the effectiveness of precipitation strengthening. In the RCR steels, VC was not present in the austenite during rolling as shown by the solubility product curve in Fig. 9. VC precipitation occurs at temperatures lower than the finish rolling temperature, 850 °C, and thus is not a major strengthening mechanism in the RCR condition.

In order to show the potential contribution of precipitate strengthening in each alloy, Ashby-Orowan strengthening increment calculations and the maximum precipitate volume fraction attainable for each alloy are presented in Fig. 10. The maximum precipitate volume fraction attainable in each experimental steel can be derived using the procedure outlined by Gladman (Ref 23) and is shown by dotted lines on Fig. 10. The maximum volume fraction and thus, largest possible strengthening increment provided by the NbC in the RA/Q steels is less than that of the CR steel; a strengthening increment of 100 MPa is possible for the RA/Q steels compared to 130 MPa for the CR steels. Even though there is greater precipitation strengthening potential in the CR steels, the strength of the RA/Q materials is comparable to the CR steels. Therefore, it is likely that the magnitude of precipitation strengthening is minor compared to strengthening due to martensite block boundaries The precipitation strengthening potential of the VC in the RCR condition is also shown in

Fig. 10, but as mentioned previously it is unlikely there is significant precipitation strengthening in the as-quenched RCR condition. Precipitation strengthening in the RCR condition would be more prominent on tempering, which has been shown in other DQ studies on vanadium containing steels (Ref 3, 9). Even with very little precipitation strengthening potential compared to the other conditions, the strength of the RCR transverse and longitudinal specimens is equivalent or greater than the CR conditions. Overall, precipitate strengthening does not provide a major difference in strength in any of the conditions outside the range of strength deviation.

Research performed by Baker (Ref 25) has shown that deformation substructure can be retained from rolled austenite in the final microstructure. Correspondingly, there is most likely retained dislocation density in the martensite of the DQ steels due to finish rolling of the CR and RCR steels that may increase strength over that achievable in the RA/Q condition. An increase in dislocation density of 10^9 cm^{-2} corresponds to an approximately 100 MPa increase in strength in ferrite (Ref 26). The average strength of the DQ conditions is slightly higher than the RA/Q condition, especially in the transverse direction, but the deviation is within the scatter in the data. Since there should not be additional precipitate strengthening in the RCR condition compared to the CR conditions but its strength was comparable to the upper range of strength in the CR conditions, any strength increase of the DQ CR or RCR conditions over the RA/Q appears to be mostly attributable to retained deformation substructure. The amount of finish rolling reduction did not greatly change the strength of the CR condition specimens, suggesting that the amount of retained work was not significantly different within the range of rolling reductions that were assessed.

4. Summary and Conclusions

The microstructure and mechanical properties were measured for martensitic plate steels subjected to several different TMCP routes including direct quenching and reaustenitizing and quenching. The objective of the investigation was to assess the microstructure evolution and corresponding strengthening mechanisms due to various TMCP routes. Based on the results of the work, the following conclusions have been reached:

(1) Although the PAGS and morphology varied among the conditions examined, the martensitic microstructure size scale is not significantly different for the processing conditions assessed. Specifically, the martensitic block sizes are comparable, which is important because martensite blocks are the smallest microstructural units with high-angle grain boundaries.
(2) The tensile properties of the CR conditions were independent of the amount of finish rolling reduction, implying that strengthening due to deformation substructure was comparable between the conditions. Similarly, the strength of the RCR condition, which had a mixture of recrystallized and deformed austenite grains, was comparable, indicating that inherited dislocations in martensite from austenite processing produced similar amounts strengthening across the DQ processing conditions assessed.
(3) The relatively constant strength between the conditions may be at least partly attributed to the constancy of martensite block size between the conditions. The contributions of the other strengthening mechanisms did not produce differences outside the range of deviation in the strength data.

Acknowledgments

The authors gratefully acknowledge the support of the Advanced Steel Products and Processing Research Center (ASPPRC), a joint industry university cooperative research center at the Colorado School of Mines. Dr. Denqgi Bai, of SSAB Americas, provided useful discussion of plate steel recrystallization behavior. ArcelorMittal and U.S. Steel very graciously provided experimental steel heats and rolling facilities respectively in support of the project.

References

1. K. Taylor and S.S. Hansen, Structure and Properties of Some Directly-Quenched Martensitic Steels, *Proceedings of the International Symposium on Accelerated Cooling of Rolled Steel*, G.E. Ruddle and A.F. Crawley, Ed., Pergamon Press, 1987, p 85–101
2. T. Swarr and G. Krauss, The Effect of Structure on the Deformation of As-Quenched and Tempered Martensite in an Fe-0.2 pct C Alloy, *Metall. Mater. Trans. A.*, 1976, **7**, p 41–48
3. R.K. Weiss and S.W. Thompson, Strength Differences Between Direct-Quenched and Reheated-and-Quenched Plate Steels, *Physical Metallurgy of Direct-Quenched Steels*, S.W. Thompson, K.A. Taylor, and F.B. Fletcher, Ed., TMS, 1993, p 107-158
4. R.P. Foley and G. Krauss, Tempering Response of Direct-Quenched and Reheat-and-Quenched Low-Carbon Martensitic Steels, *Heat Treating Including Steel Heat Treating in the New Millenium: An International Symposium in Honor of Professor George Krauss*, G. Krauss, S.J. Midea, and G.D. Pfaffmann, Ed., ASM International, Materials Park, OH, 1999, p 646–654
5. G. Krauss and C.J. McMahon, Jr., Low-Toughness and Embrittlement Phenomena in Steels, *Martensite*, G. Olson and W. Owen, Ed., ASM International, Materials Park, OH, 1992, p 295–321
6. K. Taylor, Method for Measuring the Hardenability of Direct-Quenched Plate Steels, *Heat Treatment and Surface Engineering: New Technology and Practical Applications*, G. Krauss, Ed., ASM International, Materials Park, OH, 1988, p 137–142
7. W. Schutz, H.J. Kirsch, P. Fluss, and V. Schwinn, Extended Property Combinations in Thermomechanically Control Processed Steel Plates by Application of Advanced Rolling and Cooling Technology, *Ironmak. Steelmak.*, 2001, **28**, p 180–184
8. K.E. Easterling and A.R. Tholen, The Nucleation of Martensite in Steel, *Acta Metall.*, 1976, **24**, p 333–341
9. K.A. Taylor and S.S. Hansen, Effects of Vanadium and Processing Parameters on the Structures and Properties of a Direct-Quenched Low-Carbon Mo-B Steel, *Metall. Mater. Trans. A.*, 1991, **22**, p 2359–2374
10. H. Morikawa and T. Hasegawa, Microstructures and Strengthening Factors of Accelerated Cooled Steel, *Accelerated Cooling of Steel*, P.D. Southwick and A.J. Deardo, Ed., TMS, Warrendale, 1985, p 83–96
11. R. Weiss, Ph.D. Thesis, Colorado School of Mines, 1994
12. S. Morito, X. Huang, T. Furuhara, T. Maki, and N. Hansen, The Morphology and Crystallography of Lath Martensite in Alloy Steels, *Acta Mater.*, 2006, **54**, p 5323–5331
13. S. Morito, H. Yoshida, T. Maki, and X. Huang, Effect of Block Size on the Strength of Lath Martensite in Low Carbon Steels, *Mat. Sci. Eng. A Struct.*, 2006, **438**, p 237–240
14. F. Boratto, R. Barbosa, S. Yue, and J.J. Jonas, Effect of Chemical Composition on the Critical Temperatures of Microalloyed steels, *THERMEC-88*, ISIJ, 1988, p 383–390
15. F. Fletcher, *Austenite Processing Symposium* (Internal ArcelorMittal Presentation), Paris, France, 2008
16. K. Irvine, F. Pickering, and T. Gladman, Grain-Refined C-Mn Steels, *J. Iron Steel I*, 1967, **205**, p 161–182

17. B.R. Morris, A.M. Gokhale, and G.F. Vander Voort, Grain Size Estimation in Anisotropic Materials, *Metall. Mater. Trans. A.*, 1998, **29**, p 237–244
18. A.J. Baddeley, H.J. Gundersen, and L.M. Cruz-Orive, Estimation of Surface Area from Vertical Sections, *J. Microsc.*, 1986, **142**, p 259–276
19. ASTM Standard E8, ASTM International, West Conshohocken, PA, 2008
20. D. Bai, R. Bodnar, J. Ward, J. Dorricott, and S. Sanders, *International Symposium on Recent Developments in Plate Steels*, AIST, p 13–22
21. A.J. Kaijalainen, P.P. Suikkanen, L.P. Karjalainen, J.I. Kömi, and A.J. DeArdo, Effect of Austenite Conditioning in the Non-recrystallization Regime on the Microstructures and Properties of Ultra High Strength Strip Steel with Bainitic/Martensitic Microstructures, *2nd International Conference on Super-High Strength Steels*, Peschiera del Garda, Italy, 2010
22. J. Morris, Comments on the Microstructure and Properties of Ultrafine Grained Steel, *ISIJ Int.*, 2008, **48**, p 1063–1070
23. T. Gladman, *The Physical Metallurgy of Microalloyed Steels*, Maney Publishing for the Institute of Materials, London, England, 1997
24. S.S. Hansen, J.B.V. Sande, and M. Cohen, Niobium Carbonitride Precipitation and Austenite Recrystallization in Hot-Rolled Microalloyed Steels, *Metall. Mater. Trans. A.*, 1980, **11**, p 387–402
25. T.N. Baker, Subgrain and Dislocation Strengthening in Controlled-Rolled Microalloyed Steels, *Hot Working and Forming Processes*, C.M. Sellars and G.J. Davies, Ed., Maney Publishing, Sheffield, London, England, 1980, p 32–37
26. B.C. De Cooman, J.G. Speer, I.Y. Pyshmintsev, and N. Yoshinaga, *Materials Design: The Key to Modern Steel Products*, Grips Media GmbH, Bad Harzburg, Germany, 2008